Fluorinated carbon as high-performance cathode for aqueous zinc primary batteries

Congping Xu[a, b, c], Liang Zhang [d], Fupeng Liu*[a], Ruding Zhang*[b, c], Hongjun Yue*[b, c]

[a] Faculty of Materials Metallurgy and Chemistry, Jiangxi University of Science and Technology, Ganzhou 341000 Jiangxi, China

[b] CAS Key Laboratory of Design and Assembly of Functional Nanostructures, and Fujian Provincial Key Laboratory of Nanomaterials, Fujian Institute of Research on the Structure of Matter, Chinese Academy of Sciences, Fuzhou 350002, China

[c] Xiamen Institute of Rare-earth Materials, Haixi Institutes, Chinese Academy of Sciences, Xiamen 361021, China

[d] State Key Laboratory of Advanced Chemical Power Sources, Guizhou Meiling Power Sources Co.Ltd., Zunyi 563003, China

* Corresponding authors

E-mail address:

fupengliu@126.com; rdzhang@fjirsm.ac.cn; hjyue@fjirsm.ac.cn

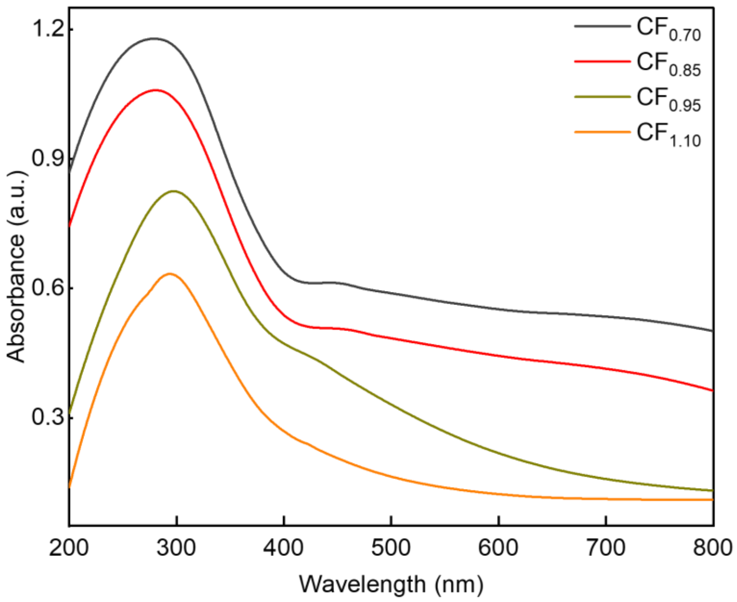

Fig. S1. UV-Vis spectra of the CF_x powder.

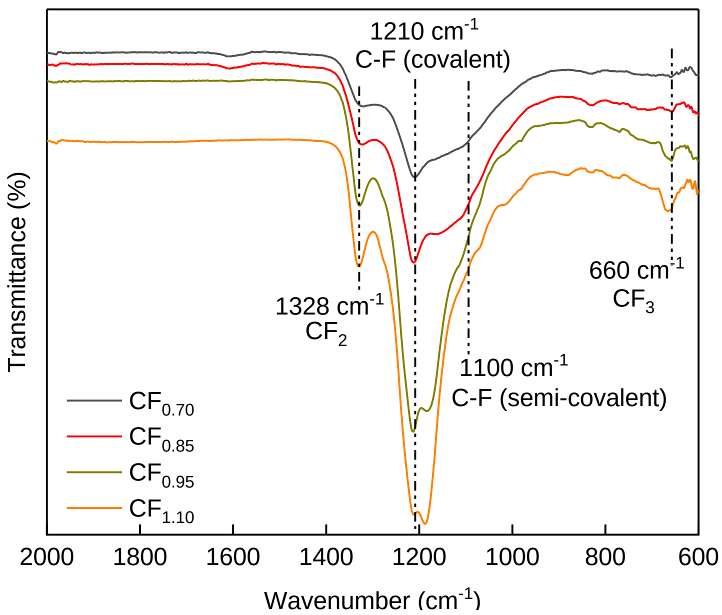

Fig. S2. IR absorption spectra of the CF_x.

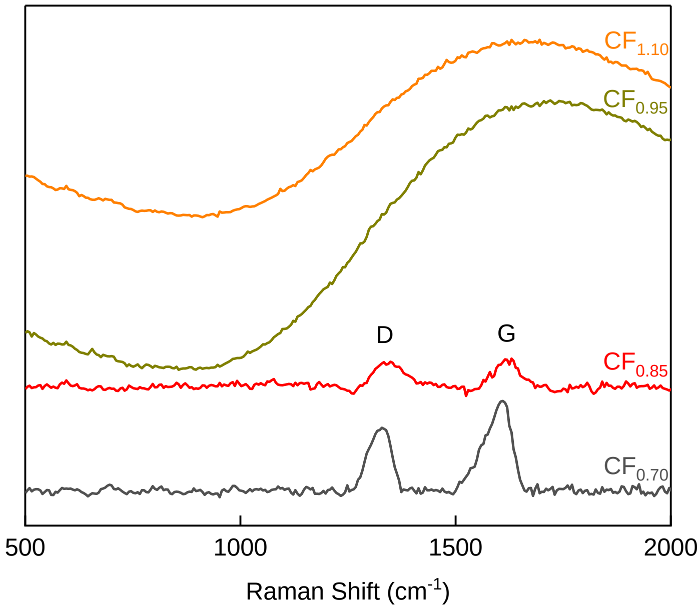

Fig. S3. Raman spectra of the CF_x.

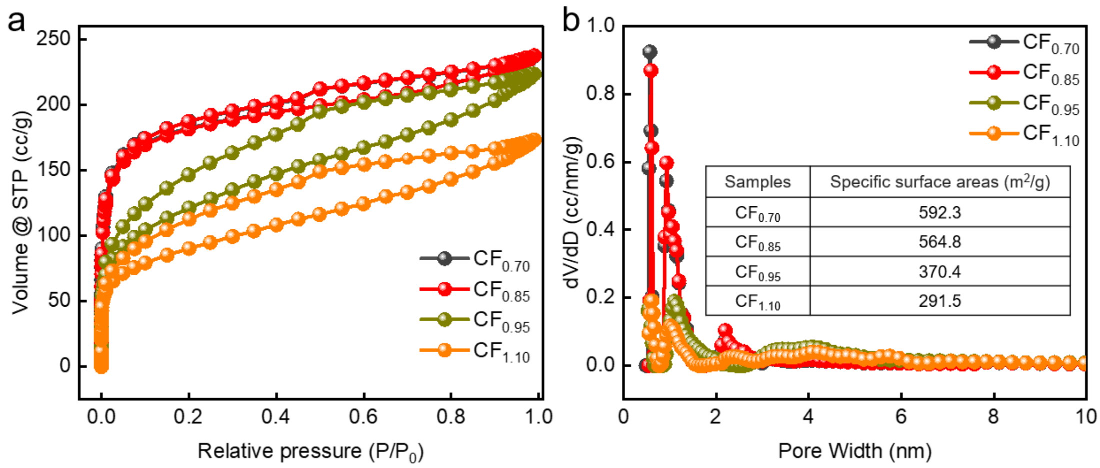

Fig. S4. (a) Nitrogen isotherms and (b) pore size distributions of CF_x. Illustration shows specific surface area.

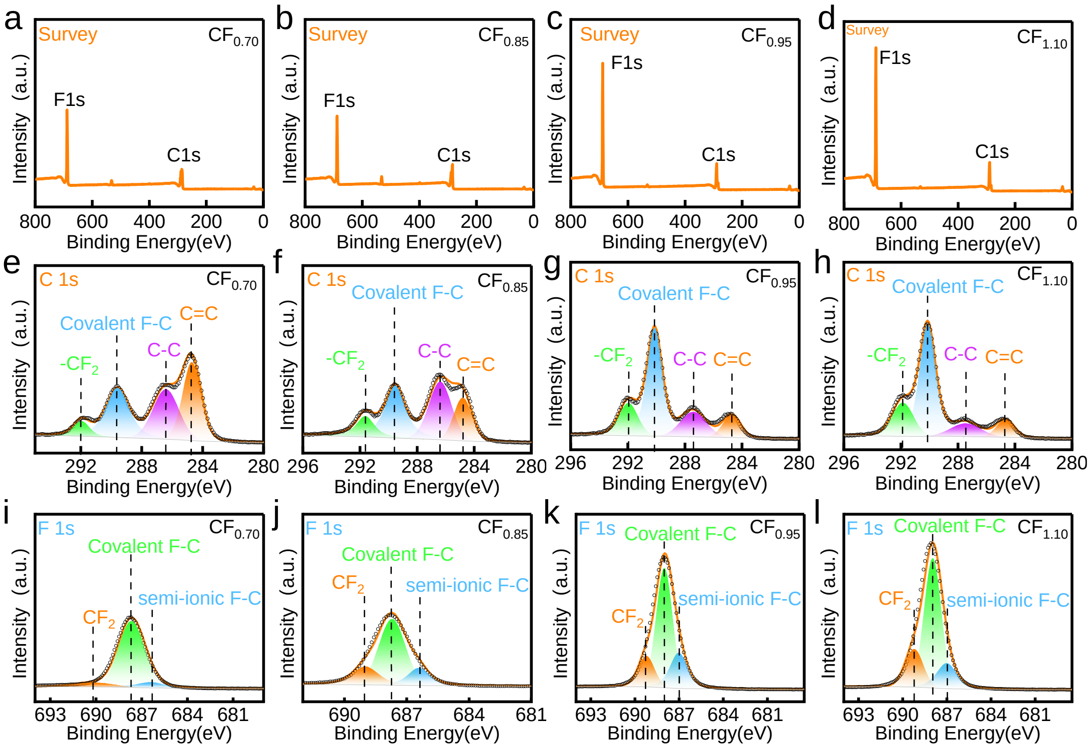

Fig. S5. The XPS survey spectra of CF_x (a-d). High resolution C 1s (e–h) and F 1s (i–l) spectra of CF_x.

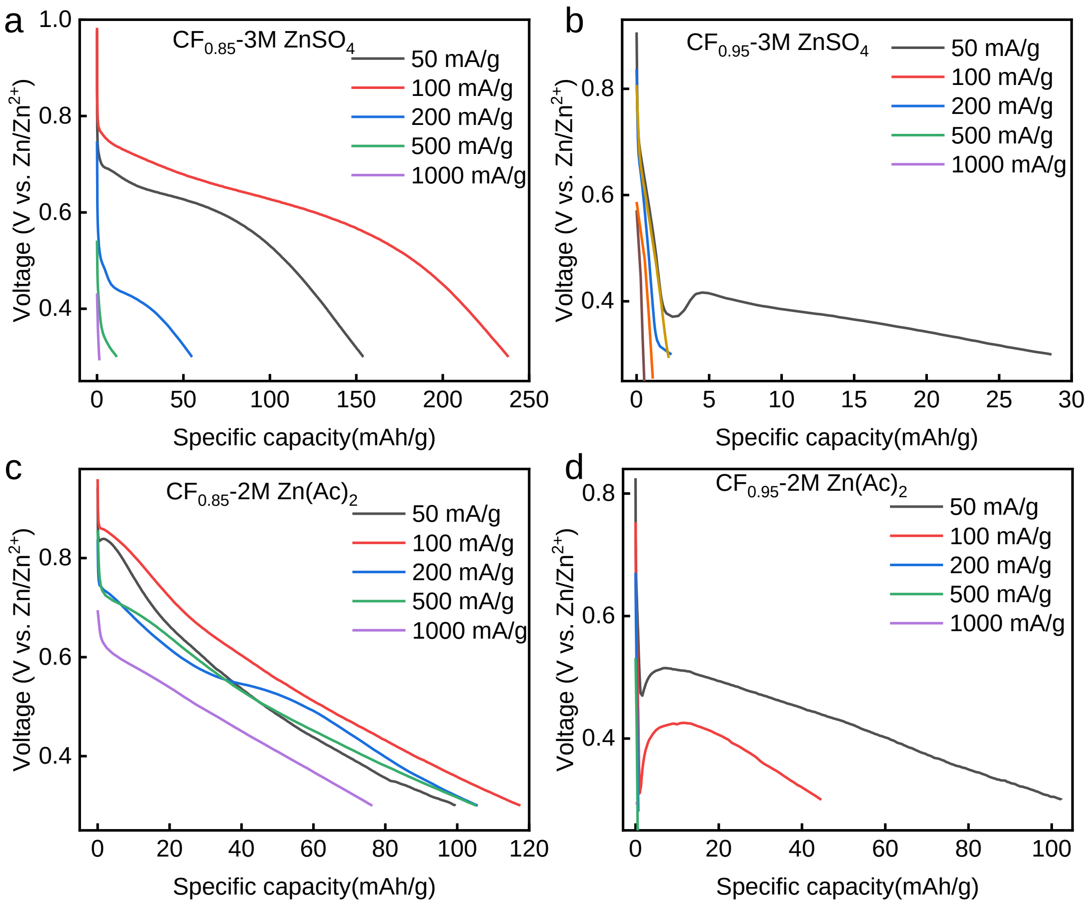

Fig.S6. Discharge curves of Zn/$CF_{0.85}$, Zn/$CF_{0.95}$ with (a) and (b) zinc sulfate, (c) and (d) zinc acetate as electrolyte.

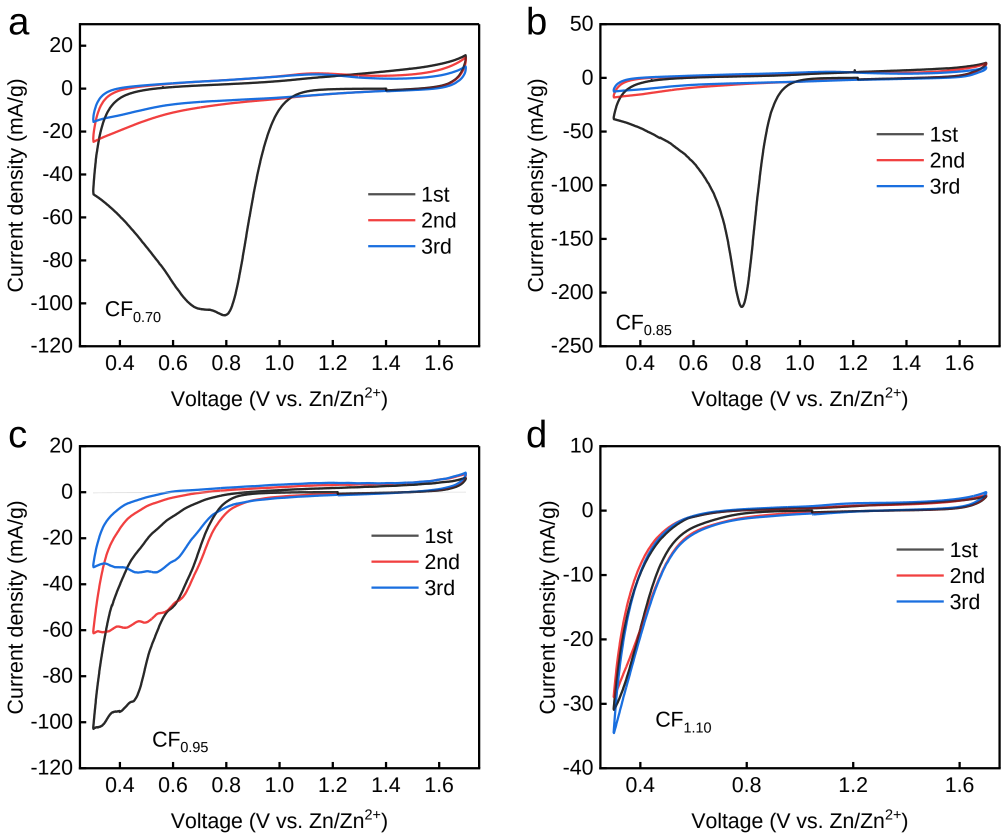

Fig.S7. CV profiles of the CF_x at a scan rate of 0.1 mV/s in aqueous $Zn(OTf)_2$ (a)$CF_{0.70}$, (b) $CF_{0.85}$, (c) $CF_{0.95}$, (d) $CF_{1.10}$.

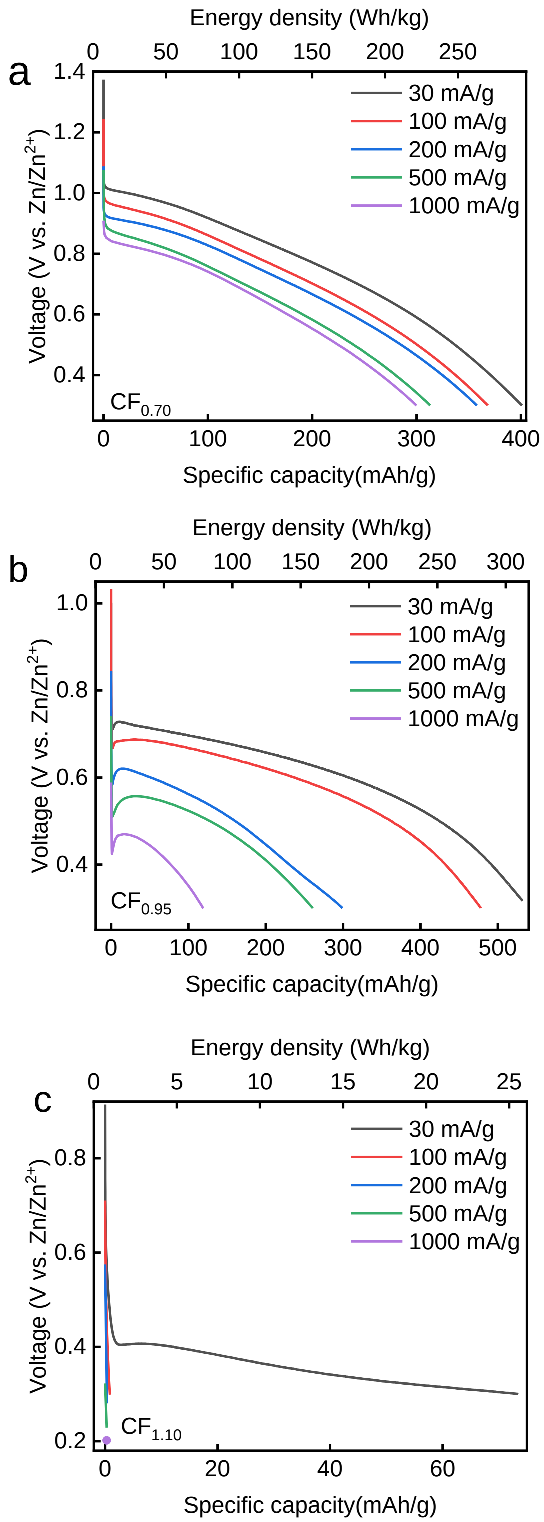

Fig.S8. Galvanostatic discharge plots of the (a) Zn/$CF_{0.70}$, (b) Zn/$CF_{0.95}$, (c) Zn/$CF_{1.10}$ battery at different rates.

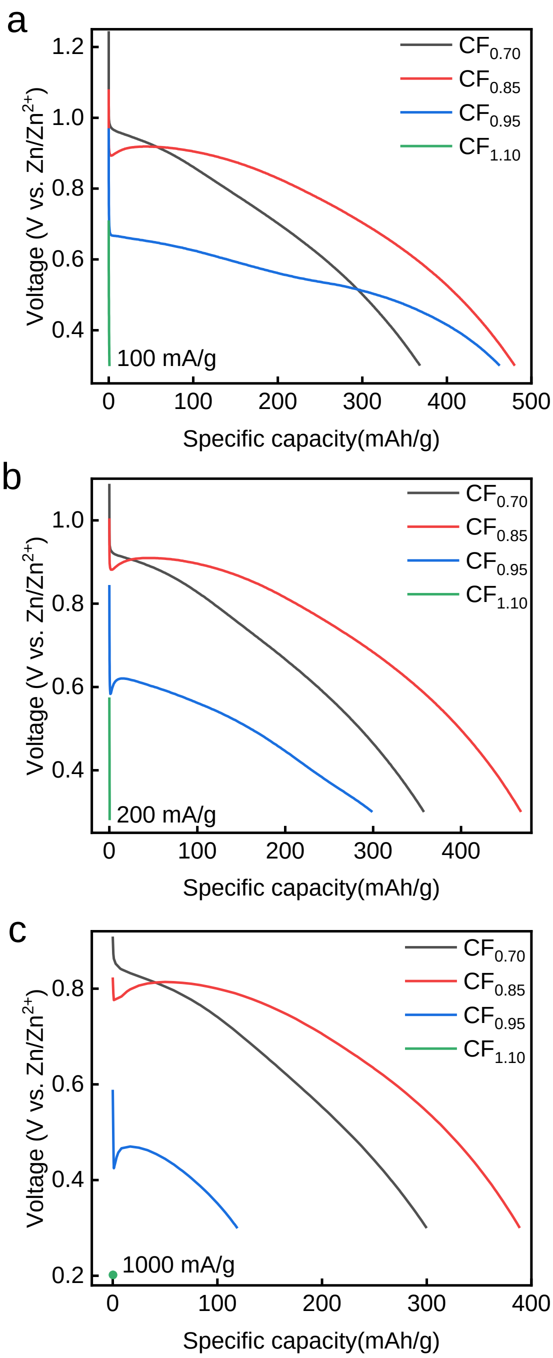

Fig.S9. Comparison of discharge curves of CF_x at the 25 °C (a)100 mA/g, (b) 200 mA/g and (c) 1000 mA/g.

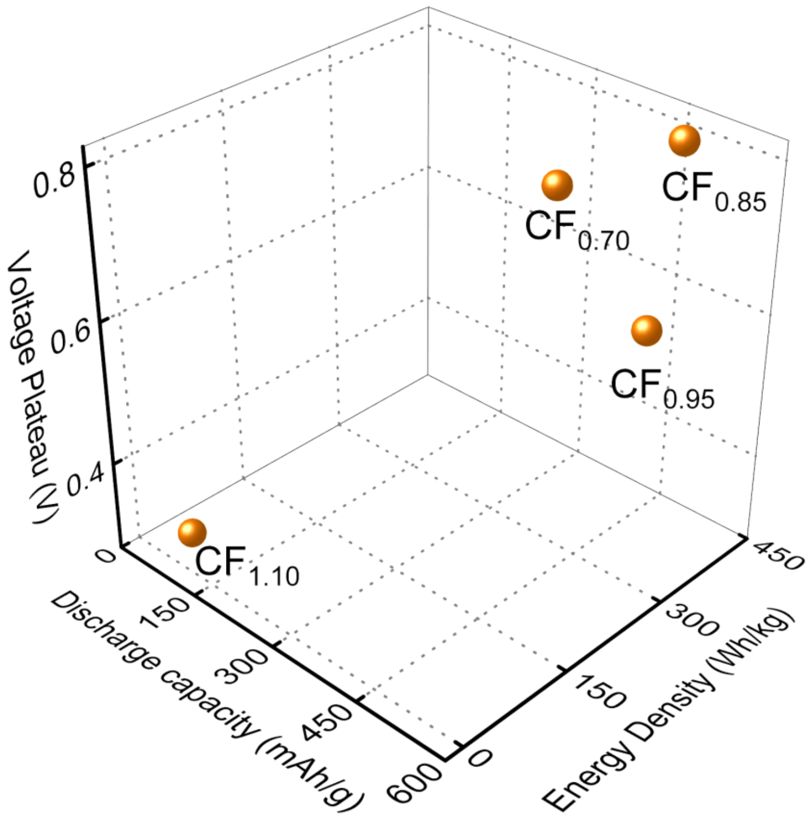

Fig.S10. Energy density, discharge capacity, and the corresponding voltage plateau of CF_x at 30 mA/g.

Table S1. Discharge capacity, Energy density and mid-voltage of CF_x at various current density and 25 ℃.

	30 mA/g			100 mA/g			200 mA/g			500 mA/g			1000 mA/g		
	C	E	V	C	E	V	C	E	V	C	E	V	C	E	V
$CF_{0.70}$	401	297	0.77	368	259	0.73	358	243	0.70	313	201	0.66	300	189	0.65
$CF_{0.85}$	503	388	0.81	480	352	0.78	458	339	0.77	425	293	0.74	389	258	0.72
$CF_{0.95}$	532	317	0.62	462	247	0.54	299	147	0.51	261	124	0.49	119	49	0.43
$CF_{1.10}$	73.5	26.1	0.35	0.86	0.36	0.39	0.33	0.14	0.42	0.27	0.07	0.32	0.28	0.05	0.20

C denotes Capacity (mAh/g), E denotes Energy density (Wh/kg), V denotes Mid-voltage (V).

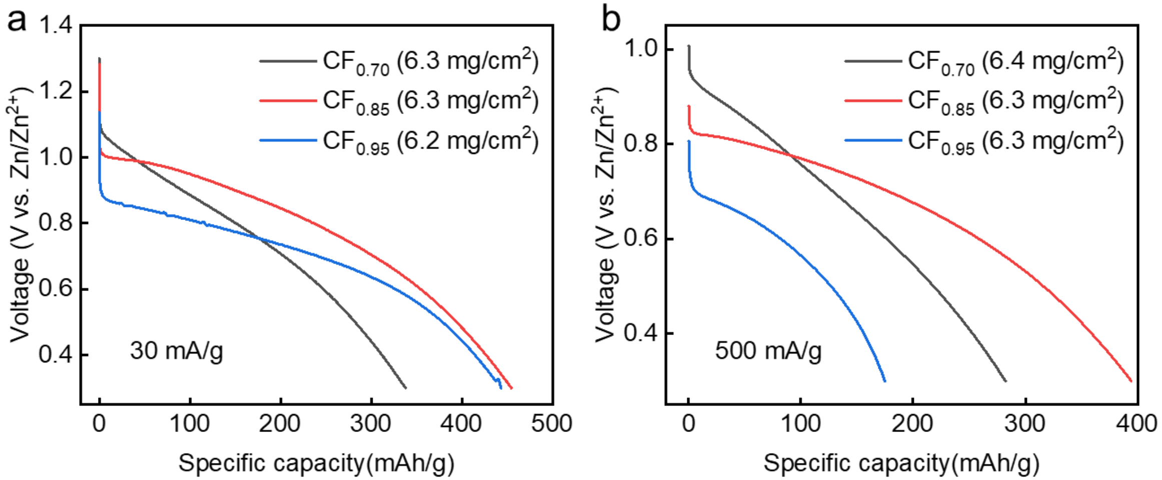

Fig.S11. Galvanostatic discharge curves of CF_x discharged with high mass loading.

Table S2. Discharge capacity, Energy density and mid-voltage of CF_x with high mass loading.

	30 mA/g			500 mA/g		
	C	E	V	C	E	V
$CF_{0.70}$	338	251	0.77	282	186	0.67
$CF_{0.85}$	455	348	0.81	394	254	0.68
$CF_{0.95}$	443	303	0.72	175	99	0.59

C denotes Capacity (mAh/g), E denotes Energy density (Wh/kg), V denotes Mid-voltage (V).

Table S3. Comparison with primary cells reported in the literature.

Kinds of batteries	Constructions		Voltage (V)	Capacity (mAh/g)	Energy density (Wh/kg)	Reaction mechanism	References
	Electrolyte	Cathode					
Zn/CF_x	$Zn(CF_3SO_3)_2$	CF_x	1.0	503	388	$2CF_x+xZn^{2+}+xZn+2xH_2O\rightarrow 2C+2xZnOHF+2xH^+$	This work
Zn/MnO_2	KOH	MnO_2	1.2	224	234	$Zn+MnO_2+2H_2O+2KOH\rightarrow Mn(OH)_2+K_2[Zn(OH)_4]$	1
Zn/HgO	KOH	HgO	1.2	190	266	$Zn+HgO=ZnO+Hg$	2
Zn/Ag_2O	KOH	Ag_2O	1.5	180	287	$Zn+Ag_2O+ H_2O\rightarrow Zn(OH)_2+2Ag$	2
Zn/O_2	NH_4Cl/ KOH	O_2	1.2	800	1350	$2Zn+O_2\rightarrow 2ZnO$	2
Mg/CF_x	APC/THF	CF_x	1.5	813	1085	$CF_x + \frac{x}{2}Mg^{2+}+xe^-\rightarrow C +\frac{x}{2}MgF_2$	3
Li/CF_x	$LiPF_6$	CF_x	2.7	922	2466	$CF_x + xLi\rightarrow C + xLiF$	4

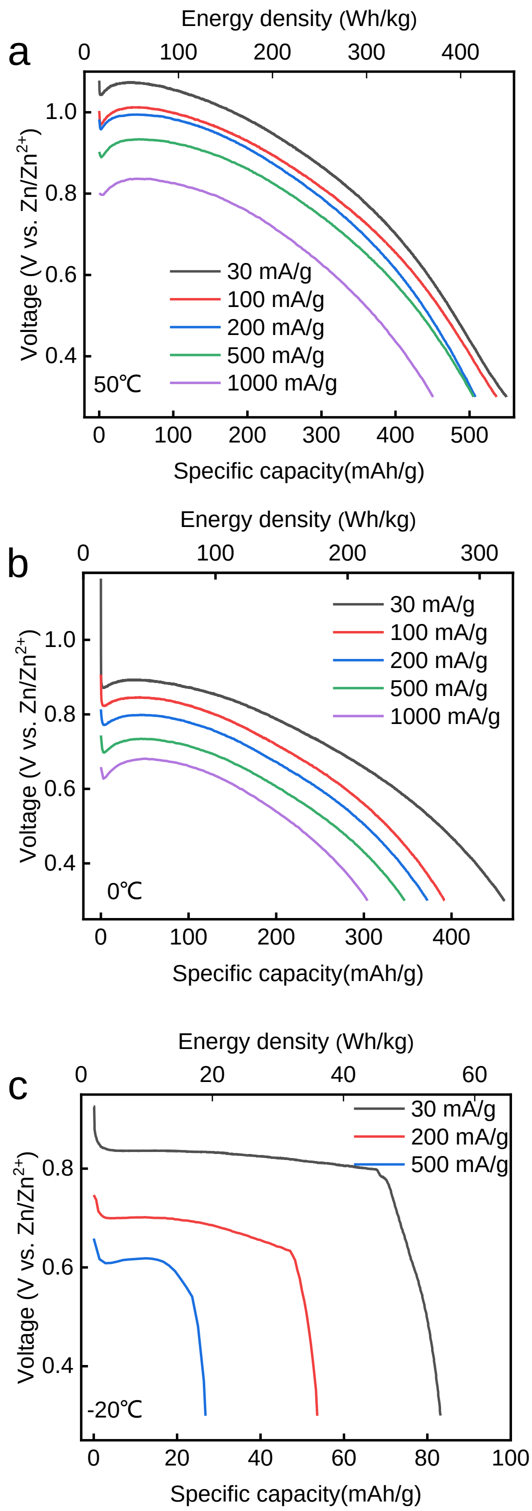

Fig.S12. Galvanostatic discharge plots of the $Zn/CF_{0.85}$ battery at (a) 50 ℃, (b) 0 ℃, (c) -20 ℃

Table S4. Discharge capacity and voltage platform of $CF_{0.85}$ at various current density and tested temperatures.

	30 mA/g				200 mA/g				500 mA/g			
	-20 ℃	0 ℃	25 ℃	50 ℃	-20 ℃	0 ℃	25 ℃	50 ℃	-20 ℃	0 ℃	25 ℃	50 ℃
Capacity (mAh/g)	83	460	503	550	54	373	468	508	27	347	425	505
Energy density (Wh/kg)	66	325	388	457	36	342	339	401	16	209	294	377
Mid-voltage (V)	0.82	0.75	0.81	0.90	0.69	0.69	0.77	0.85	0.62	0.64	0.74	0.80

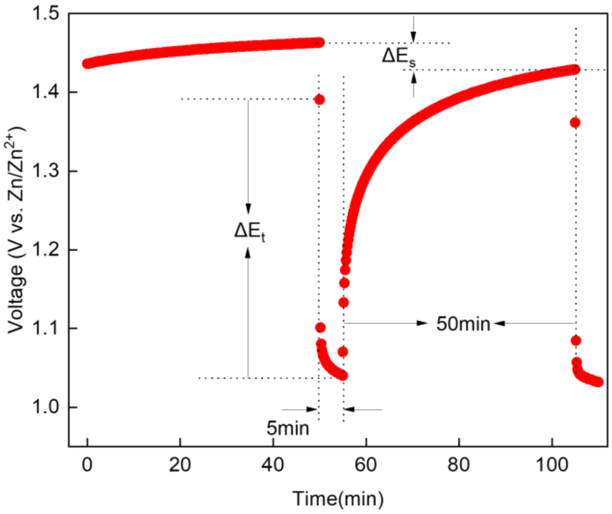

Fig. S13. Scheme for a single step of a GITT experiment.

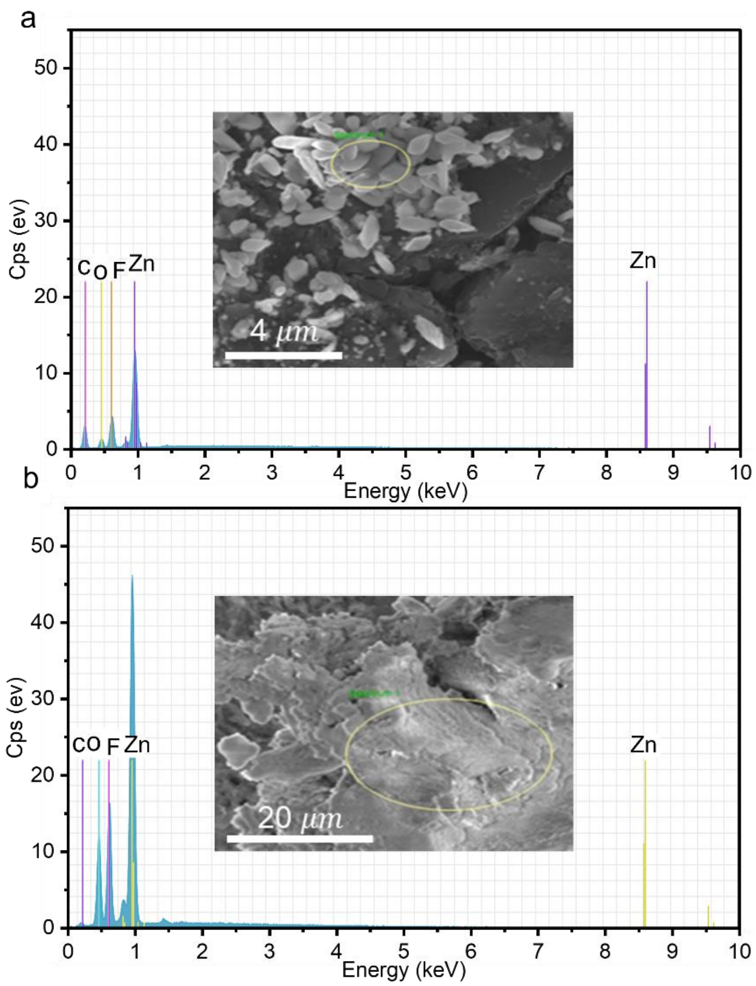

Fig.S14. EDS after discharging at 30 mA/g (a) and (b) cathode, (c) and (d) anode.

Table S5. Cathode and anode element content after discharging at 30 mA/g.

	element	C	O	F	Zn
atomic ratio	cathode	38.37	18.48	25.75	17.40
	anode	2.56	31.76	36.23	29.44

References

1. D. Linden, Handbook of batteries and Fuel Cell, Mc Graw-Hill, New York, 1984: Part Ⅰ,chapt.1-3
2. T. Sarakonsri and R. Vasant Kumar, *Rechargeable Ion Batteries: Materials, Design and Applications of Li-Ion Cells and Beyond*, 2023, 21-47.
3. X. Miao, J. Yang, W. Pan, H. Yuan, Y. Nuli and S.-i. Hirano, *Electrochimica Acta*, 2016, **210**, 704-711.
4. C. Peng, Y. Li, F. Yao, H. Fu, R. Zhou, Y. Feng and W. Feng, *Carbon*, 2019, **153**, 783-791.